

Percolation transitions in bilayer graphene encapsulated by hexagonal boron nitride

C. Cobaleda,^{1,*} S. Pezzini,^{1,2} A. Rodriguez,³ E. Diez,¹ and V. Bellani²

¹Laboratorio de Bajas Temperaturas, Universidad de Salamanca, E-37008 Salamanca, Spain

²Dipartimento di Fisica, Università degli studi di Pavia, I-27100 Pavia, Italy

³Physikalisches Institut, Albert-Ludwigs-Universität Freiburg, Hermann-Herder-Straße 3, D-79104, Freiburg, Germany

(Received 15 April 2014; revised manuscript received 13 October 2014; published 27 October 2014)

We studied the plateau-plateau transitions that characterize the electrical transport in the quantum Hall regime in a high mobility bilayer graphene flake encapsulated by hexagonal boron nitride at magnetic fields up to 9 T and temperatures above 300 mK. We measured independently the exponent κ of the temperature-induced transition broadening, the critical exponent γ of the localization length, and the exponent p ruling the temperature scaling of the coherence length, finding consistency with the relation $\gamma = p/2\kappa$. The observed value of $\kappa = 0.30(0.28, 0.32)$ deviates from that of the quantum Hall critical point. The obtained $\gamma = 1.25(0.96, 1.54)$ questions the validity of a pure Anderson transition, and reveals percolation as the underlying driving mechanism.

DOI: [10.1103/PhysRevB.90.161408](https://doi.org/10.1103/PhysRevB.90.161408)

PACS number(s): 72.80.Vp, 73.43.Qt

Quantum phase transitions appear frequently in physics, in superconductors, optical lattices, two-dimensional (2D) materials, etc., presenting significant implications across these physics fields. One main point that is still an open question concerns electron transport in two dimensions in the presence of disorder, and experimental efforts are underway to take a crucial step toward understanding the interplay of disorder and the interaction between the electrons. It is known that the plateaus of the Hall resistivity (ρ_{xy}) in the quantum Hall regime correspond to localized states, whereas between two adjoining plateaus there is an extended state at a critical magnetic field (B_c) [1]. The plateau-plateau transition (PPT) (between two contiguous plateaus) is a localization-delocalization transition characterized by the exponent γ controlling the divergence of the localization length, $\xi \propto |B - B_c|^{-\gamma}$ [2,3]. This power law results in a temperature-induced broadening of the PPT, i.e., $(d\rho_{xy}/dB)_{\max} \propto T^{-\kappa}$ [2,4], where $\kappa = p/2\gamma$ and p determines the scaling of the inelastic scattering (coherence) length $L_\phi \propto T^{-p/2}$. The first estimates of γ , made in the absence of an electron-electron (e - e) interaction, led to $\gamma \sim 2.4$ (see Ref. [5] and references therein). Recently, more accurate calculations yielded $\gamma \approx 2.6$ for the noninteracting critical point [5–7]. The experimentally measured values for the PPT exponents in a two-dimensional electron gas (2DEG) read $\kappa = 0.42$, $p = 2$, and $\gamma = 2.38$ [8,9]. It is now accepted that noninteracting models cannot describe the observed integer quantum Hall critical point (IQHCP) [10]. Besides the role of the e - e interaction, the effect of the nature of disorder on the PPT has also been partially unraveled [11]. The IQHCP is realized in the presence of short-range disorder, when Anderson physics dominates the transition. For long-range disorder, however, the PPT may be partially governed by percolation, characterized by a different set of exponents. While deviations in the value of κ , due to long-range disorder, have been observed [11], the experimental observation of a PPT fully driven by an ideal percolation mechanism still needs to be reported.

Recently, a few works have focused on the measurement of PPT critical exponents in graphene [12–14]. Nonetheless,

PPTs have not been observed in bilayer graphene, mainly due to its low mobility when placed on a standard SiO₂ substrate. However, high mobilities can be achieved by placing the graphene flake on top of hexagonal boron nitride (h -BN) [15–19]. Furthermore, the h -BN layer gives rise to an ultraflat configuration of the graphene sheet, exhibiting smooth energetic disorder and little charge inhomogeneity, as revealed by tunneling microscopy [20,21]. Graphene on h -BN thus appears as an ideal system to investigate the influence of long-range disorder on the PPT. In this Rapid Communication we measured the critical exponents κ and γ in bilayer graphene (encapsulated by h -BN) for a number of PPTs, both for negatively and positively charged carriers. We determined the exponents independently, from the scaling of the Hall conductivity, and from the analysis of the longitudinal conductivity in the regime of variable range hopping, respectively. Additionally, we estimated L_ϕ and p from the low-field weak-localization (WL) correction to the conductivity. The observed value of κ deviates from that of the IQHCP and the obtained γ is fully compatible with a classical percolation transition, and consistent with the relation $\gamma = p/2\kappa$.

These results can lead to the conception of experiments aimed at exploring the quantum phase transitions in two dimensions in different artificial potential landscapes, such as the moiré periodic potential that can be created and controlled in slightly twisted graphene/ h -BN stacks [22]. This could also open the avenue to further research for the investigation of the relevance of the quantum phase transitions and percolation in other phenomena of condensed matter physics, for instance, the quantum percolation in cuprate high-temperature superconductors [23].

The sample studied is a van der Waals heterostructure consisting in a stacking of h -BN, bilayer graphene, and h -BN, produced using the dry transfer technique described in Ref. [24]. In order to have the highest experimental accuracy, the sample under study was etched in the geometry of a Hall bar with a width over length ratio (W/L) equal to 1/6. In order to avoid large density gradients along the sample [25,26], the size of the sample was purposely small (length $\approx 6 \mu\text{m}$).

The electrical contacts were patterned by evaporation of titanium and gold and a back gate contact was also connected

*Present address: NEST, Scuola Normale Superiore and Istituto Nanoscienze–CNR, Piazza S. Silvestro 12, I-56127 Pisa, Italy.

in order to tune the carrier density. To avoid breaking the dielectric (which would result in current leakage) the back gate voltage (V_g) was not increased above 35 V. The sample was cooled down in a cryo-free refrigerator and the measurements were taken using the standard dc lock-in technique at a frequency of ~ 15 Hz with an excitation current of 10 nA obtained by applying a voltage drop of 5 V on a 500 M Ω resistor. First, we characterized the sample at 290 mK by measuring the resistance as a function of V_g in the absence of magnetic field [27]. In Fig. 1 we present the corresponding data, which show the presence of the charge neutrality point (CNP) at 0.4 V. We obtained the carrier density at different V_g from the dependence of the Hall resistance on the magnetic field (B): The electron (or hole) density is given by $n = 1/se$ at low magnetic fields, where $e > 0$ denotes the elementary charge and $s = d\rho_{xy}/dB$. The Hall mobility of this sample varied from $\mu \simeq 3.2 \times 10^4$ cm 2 V $^{-1}$ s $^{-1}$ at a carrier density $n \simeq 2 \times 10^{11}$ cm $^{-2}$ to $\mu \simeq 4.3 \times 10^4$ cm 2 V $^{-1}$ s $^{-1}$ for $n \simeq 10^{12}$ cm $^{-2}$. These values of mobility are among the highest reported values for supported bilayer graphene.

In the presence of a magnetic field, we measured simultaneously the two Hall and two longitudinal resistances, finding no substantial differences in the measurements. The fact that the two measured Hall resistances have the same quantitative behavior proves that the density on both extremes of the Hall bar is nearly the same. Thus the density gradients along the sample are negligible [26], revealing the high quality of the sample.

Figure 2 shows the isotherms of the longitudinal resistivity (ρ_{xx}) and of the Hall resistivity (ρ_{xy}) near the quantum phase transitions as a function of B at different carrier densities. In Figs. 2(a)–2(f) we observe the typical features of the IQHE in bilayer graphene, with a Hall resistance which is quantized following the relation $\rho_{xy} = h/\nu e^2$ with $\nu = \pm 4, \pm 8 \pm 12, \dots$ due to the valley and spin degeneracy. In the transient between the quantum Hall plateaus all the isotherms of ρ_{xy} acquire

the same value at a critical field B_c . Accordingly, between the extremes of the Shubnikov–de Haas oscillations there is a magnetic field at which the ρ_{xx} isotherms cross. This behavior is observed at temperatures ranging from 0.3 to 50 K, and is characteristic of a PPT [9].

In Fig. 2(g) we plot the values of $(d\rho_{xy}/dB)_{\max}$ versus temperature in a log-log scale for the observed PPTs at different densities. The data show a saturation temperature of ~ 5 K and become independent of T below this value. This effect is due to the finite size of the sample. Since the coherence length increases with decreasing temperature ($L_\phi \propto T^{-p/2}$), we expect that at low enough T the value of L_ϕ becomes comparable to the Hall bar width ($W = 1$ μ m), which is the smallest dimension of the sample. At this point the dominant length scale will be W itself rather than L_ϕ , which gives rise to the saturation observed. (In this sense one can see L_ϕ as a T -dependent effective size of the sample [8].) The saturation of the coherence length is confirmed by the values of $L_\phi(T)$ that we obtained from weak-localization (WL) measurements, which are shown in the inset of Fig. 3. The latter inset shows the magnetoconductivity measured for small fields ($|B| \leq 12$ mT) at different temperatures, which evidence pronounced dips due to WL. From the best fit to the magnetoconductivity—using the theoretical approach described in Ref. [28]—we determine L_ϕ at each temperature [29], as shown in Fig. 3. Below 5 K, the coherence length approaches 1 μ m and the power law behavior is clearly lost.

Having understood the observed saturation phenomenon, we proceed to characterize the critical exponent κ of the PPTs, using only the data at $T \geq 5$ K. From the linear fit of the values of $(d\rho_{xy}/dB)_{\max}$ shown in Fig. 2(g), we obtain κ for several transitions at different densities, as summarized in Table I. As we can see, $0.27 \leq \kappa \leq 0.32$ independently of either the density or the Landau level indices of the transition. From the sample mean of the set we estimate the critical exponent to be

$$\kappa = 0.30(0.28, 0.32), \quad (1)$$

where the values in parentheses denote the 95% confidence interval [30]. This κ value is, within the estimated confidence interval, distinctly different from that typically associated with an Anderson-type transition, namely, $\kappa \simeq 0.42$, as confirmed recently in monolayer graphene [14]. In order to gain a deeper understanding of the transition, we calculated the resulting value of the universal exponent γ from the relation $\gamma = p/2\kappa$. The value of p is obtained independently by fitting the dependence of L_ϕ on temperature. The best fit, shown in Fig. 3 (black line), yields

$$p = 0.90 \pm 0.02. \quad (2)$$

It is worth mentioning that previous works carried out on monolayer [31,32] and bilayer [28] graphene have found a similar value of $p \approx 1$, while in Ref. [33] in epitaxial graphene it was shown to be sample dependent with values different from 1 and 2. We can also note that the obtained p value implies a dynamic critical exponent $z = 2/p = 2.2 \pm 0.05$, in contrast to $z = 1$ observed in 2DEG [8]. The measured values of the exponents κ [Eq. (1)] and p [Eq. (2)] lead to $\gamma = 1.49(1.38, 1.59)$.

This latter result suggests a connection with the model of Trugman [34], which considers a PPT governed by a perco-

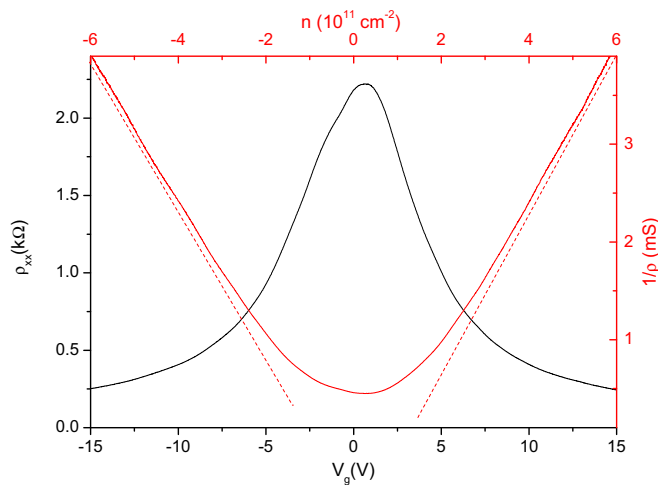


FIG. 1. (Color online) Longitudinal resistivity ρ_{xx} vs back gate voltage V_g at $T = 5$ K in the absence of magnetic field. The CNP is found to be at 0.4 V. The right axis (red) shows ρ^{-1} as a function of the carrier density n (upper abscissa axis) at $T \sim 0.3$ K. Dashed lines highlight the linear dependence of ρ^{-1} on n away from the CNP.

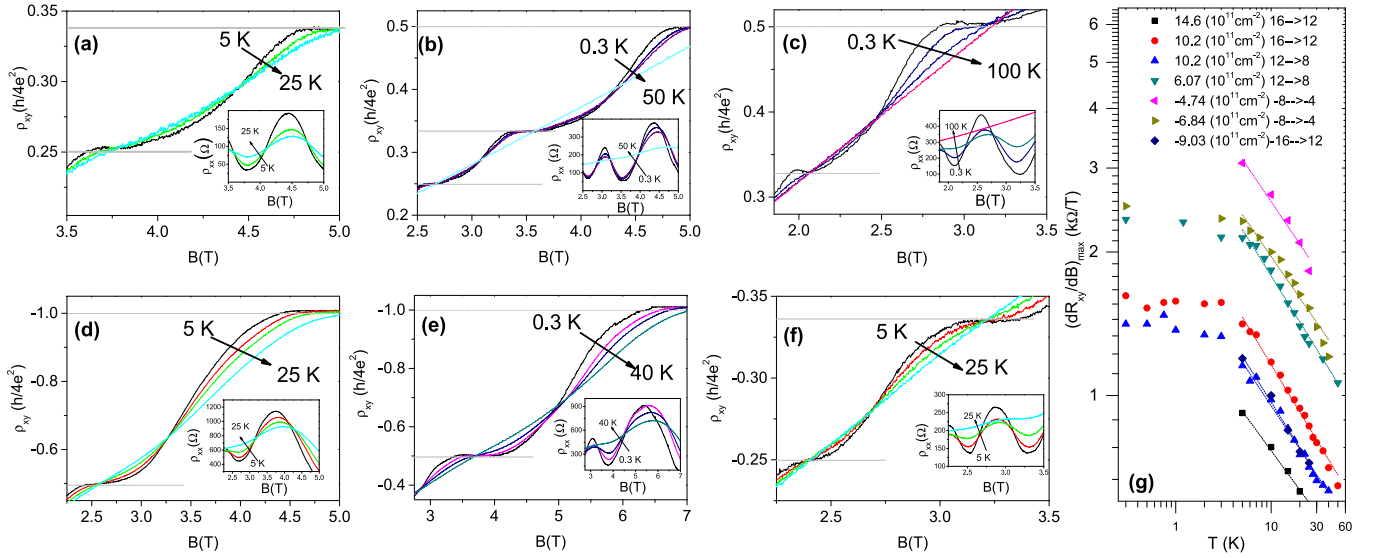


FIG. 2. (Color online) (a)–(f) show the isotherms at a few selected temperatures of the Hall resistivity ρ_{xy} as a function of the magnetic field at different densities. (a)–(c) show the QHE in the electronlike regime at densities $n = 14.6 \times 10^{11} \text{ cm}^{-2}$, $n = 10.2 \times 10^{11} \text{ cm}^{-2}$, and $n = 6.07 \times 10^{11} \text{ cm}^{-2}$, respectively. (d)–(f) show the QHE in the holelike regime at densities $n = (-)4.74 \times 10^{11} \text{ cm}^{-2}$, $n = (-)6.84 \times 10^{11} \text{ cm}^{-2}$, and $n = (-)9.03 \times 10^{11} \text{ cm}^{-2}$, respectively. The insets show the isotherms of the longitudinal resistivity ρ_{xx} as functions of the magnetic field. For clarity, gray horizontal lines indicating the values h/e^2 are included. (g) shows $(d\rho_{xy}/dB)_{\text{max}}$ as a function of the temperature in log-log scale for the PPTs displayed in (a)–(f). The estimated experimental error bars are smaller than the size of the symbols. Dashed lines correspond to linear fits of the data according to $(d\rho_{xy}/dB)_{\text{max}} \propto T^{-\kappa}$.

lation regime, for which the critical exponent is analytically known to be $\gamma = 4/3$ [35]. Another observation compatible with the existence of a percolation regime derives from the analysis of the dependence of the zero-field longitudinal conductivity on the carrier density. Following Morozov and co-workers [36], the longitudinal conductivity in graphene can empirically be expressed as $1/\rho(V_g) = 1/(\rho_L + \rho_S)$, where ρ_S is a density-independent resistivity caused mainly by short-range scattering, whereas $\rho_L^{-1} \propto n$ and is due to long-range

scattering. As we can see in Fig. 1, $1/\rho(V_g)$ changes linearly with the density away from the CNP. It can therefore be argued that $\rho_S \approx 0$, and that long-range scattering is dominant in our sample. Consequently, the underlying mechanism of the PPT might differ from that of an Anderson-type transition, whose IQH critical point is realized in the presence of short-range disorder [11].

In the search for confirmation of the percolation picture, we independently obtained the critical exponent γ by analyzing the temperature dependence of the longitudinal conductivity. For small enough $k_B T$, the conduction in the tails of the Landau levels is governed by a regime similar to variable range hopping (VRH) [37,38] and the dependence of the conductivity on temperature takes the form $\sigma_{xx} \propto e^{-\sqrt{T_0/T}}/T$. The characteristic temperature T_0 is a quantity inversely proportional to the localization length ξ , and thus close enough

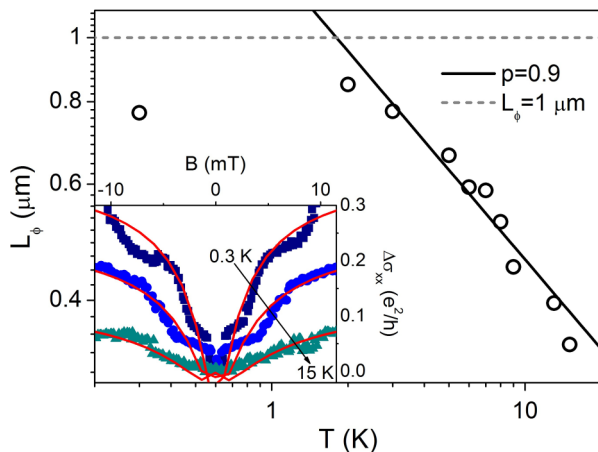


FIG. 3. (Color online) Coherence length L_ϕ as a function of temperature obtained by WL measurements at $n = 2.7 \times 10^{11} \text{ cm}^{-2}$. The best fit of the data to $L_\phi \propto T^{-p/2}$ (black line) yields $p = 0.90 \pm 0.02$, considering data for $T \geq 3 \text{ K}$. The inset shows the WL peak as a function of the magnetic field (at a set of selected different temperatures), from whose fits (red solid lines) the coherence length at each temperature is obtained [28].

TABLE I. Estimates of κ obtained from the scaling law $(d\rho_{xy}/dB)_{\text{max}} \propto T^{-\kappa}$ and the fits shown in Fig. 2(g), for different PPTs and carrier densities. Errors for κ follow from the fits and denote one standard deviation. Negative carrier densities correspond to the hole transport regime.

n (10^{11} cm^{-2})	PPT	κ
14.6	$\nu = 16 \rightarrow 12$	0.27 ± 0.01
10.2	$\nu = 12 \rightarrow 8$	0.32 ± 0.01
10.2	$\nu = 16 \rightarrow 12$	0.30 ± 0.01
6.07	$\nu = 12 \rightarrow 8$	0.32 ± 0.01
(-4.74)	$\nu = -8 \rightarrow -4$	0.30 ± 0.02
(-6.84)	$\nu = -8 \rightarrow -4$	0.29 ± 0.02
(-9.03)	$\nu = -16 \rightarrow -12$	0.32 ± 0.02

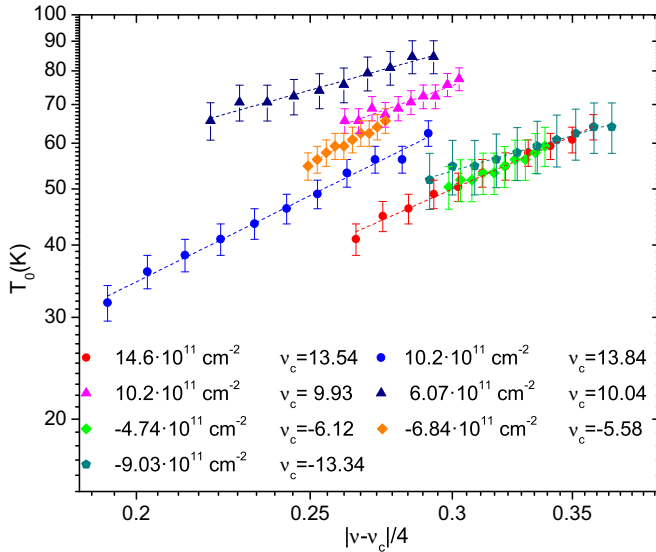


FIG. 4. (Color online) Log-log plot of the characteristic temperature T_0 of the conductivity in the tails of the Landau levels as a function of the relative filling factor for the analyzed PPTs. The factor $1/4$ in the abscissa axis is due to the fourfold degeneracy of the Landau levels. Dashed lines correspond to linear fits. The legend indicates the measured value of ν_c for the different transitions considered.

to the critical point it must scale as $T_0 \propto |\nu - \nu_c|^\gamma$, using the filling factor as the driving parameter of the transition. The latter scaling law allows for a direct estimation of γ . This approach was shown to be very well suited to access directly the scaling behavior of the localization length [39], and it has been recently adopted in the study of PPTs in monolayer graphene [14]. For a given transition and a fixed magnetic field, the value of T_0 is obtained by fitting $\sigma_{xx}(T)$ to the expression given above [40]. This procedure is carried out at different B to obtain T_0 as a function of the filling factor for the different transitions, as shown in Fig. 4. The linear fits of the latter data in a log-log plot (dashed lines in Fig. 4) provide a set of estimates for γ , whose sample mean is

$$\gamma = 1.25(0.96, 1.54). \quad (3)$$

This value is entirely compatible with a classical percolation transition, and remarkably agrees within the given confidence

interval with our previous estimate obtained from the independent measurements of the exponents κ and p . Our γ value is definitely different from the one corresponding to the interacting critical point for an Anderson-type transition, $\gamma = 2.38$, which has been found in monolayer graphene on SiO_2 [14].

In conclusion, we have measured several plateau-plateau transitions in a high mobility bilayer graphene flake encapsulated by two h -BN layers, studying the criticality of the transitions with two different approaches. The first one exploits the scaling law of the Hall resistivity, while the second is based on the analysis of the magnetoconductivity at the Landau level tails. Our results show that the transitions in this specific structure seem to be governed by a classical percolation regime, in agreement with recent theoretical results [41]. This is confirmed by a direct determination of the localization-length critical exponent γ , as well as from the estimate obtained from independent measurements of κ and the coherence length exponent p . Furthermore, the observed behavior $\rho(V_g) \propto n^{-1}$ for the zero-field resistivity indicates the existence of a dominant effective long-range scattering mechanism, compatible with a percolationlike regime. Our results are also consistent with recent experimental measurements of the profile of the energetic disorder in graphene on h -BN, revealing the existence of smooth fluctuations for the Dirac point energy [20,21].

As regards the theory that underlies the connection between quantum phase transitions, disorder, and percolation, further investigation will be devoted to the development of theoretical models that could take into account other degrees of freedom of the electrons, such as the spin polarization. The theoretical calculation will also take into account different measurement configurations, such as the nonlocal transport, that give access to specific aspects of the electronic transport in graphene [18], but can also be applied to other systems such as superconducting structures [42].

We acknowledge Dr. Niko Tombros for providing the sample and for useful discussions. This work has been supported by the Spanish MINECO MAT2013-46308-C2-1-R and FPU-AP2009-2619 (C.C.) and by the Junta de Castilla y León SA226U13. A.R. gratefully acknowledges the Deutsche Forschungsgemeinschaft (DFG) for financial support.

-
- [1] R. B. Laughlin, *Phys. Rev. B* **23**, 5632 (1981).
 - [2] A. M. M. Pruisken, *Phys. Rev. Lett.* **61**, 1297 (1988).
 - [3] F. Evers and A. D. Mirlin, *Rev. Mod. Phys.* **80**, 1355 (2008).
 - [4] S. L. Sondhi, S. M. Girvin, J. P. Carini, and D. Shahar, *Rev. Mod. Phys.* **69**, 315 (1997).
 - [5] K. Slevin and T. Ohtsuki, *Int. J. Mod. Phys.: Conf. Ser.* **11**, 60 (2012).
 - [6] K. Slevin and T. Ohtsuki, *Phys. Rev. B* **80**, 041304 (2009).
 - [7] M. Amado, A. V. Malyshev, A. Sedrakyan, and F. Dominguez-Adame, *Phys. Rev. Lett.* **107**, 066402 (2011).
 - [8] W. Li, C. L. Vicente, J. S. Xia, W. Pan, D. C. Tsui, L. N. Pfeiffer, and K. W. West, *Phys. Rev. Lett.* **102**, 216801 (2009).
 - [9] H. P. Wei, D. C. Tsui, M. A. Paalanen, and A. M. M. Pruisken, *Phys. Rev. Lett.* **61**, 1294 (1988).
 - [10] I. Burmistrov, S. Bera, F. Evers, I. Gornyi, and A. Mirlin, *Ann. Phys.* **326**, 1457 (2011).
 - [11] W. Li, G. A. Csáthy, D. C. Tsui, L. N. Pfeiffer, and K. W. West, *Phys. Rev. Lett.* **94**, 206807 (2005).
 - [12] M. Amado, E. Diez, D. Lopez-Romero, F. Rossella, J. M. Caridad, F. Dionigi, V. Bellani, and D. K. Maude, *New J. Phys.* **12**, 053004 (2010).

- [13] M. Amado, E. Diez, F. Rossella, V. Bellani, D. Lopez-Romero, and D. K. Maude, *J. Phys.: Condens. Matter* **24**, 305302 (2012).
- [14] A. J. M. Giesbers, U. Zeitler, L. A. Ponomarenko, R. Yang, K. S. Novoselov, A. K. Geim, and J. C. Maan, *Phys. Rev. B* **80**, 241411 (2009).
- [15] C. R. Dean, A. F. Young, I. Meric, C. Lee, L. Wang, S. Sorgenfrei, K. Watanabe, T. Taniguchi, P. Kim, K. L. Shepard, and J. Hone, *Nat. Nanotechnol.* **5**, 722 (2010).
- [16] A. S. Mayorov, R. V. Gorbachev, S. V. Morozov, L. Britnell, R. Jalil, L. A. Ponomarenko, P. Blake, K. S. Novoselov, K. Watanabe, T. Taniguchi, and A. K. Geim, *Nano Lett.* **11**, 2396 (2011).
- [17] R. V. Gorbachev, A. K. Geim, M. I. Katsnelson, K. S. Novoselov, T. Tudorovskiy, I. V. Grigorieva, A. H. MacDonald, S. V. Morozov, K. Watanabe, T. Taniguchi, and L. A. Ponomarenko, *Nat. Phys.* **8**, 896 (2012).
- [18] D. A. Abanin, S. V. Morozov, L. A. Ponomarenko, R. V. Gorbachev, A. S. Mayorov, M. I. Katsnelson, K. Watanabe, T. Taniguchi, K. S. Novoselov, L. S. Levitov, and A. K. Geim, *Science* **332**, 328 (2011).
- [19] L. A. Ponomarenko, A. K. Geim, A. A. Zhukov, R. Jalil, S. V. Morozov, K. S. Novoselov, I. V. Grigorieva, E. H. Hill, V. V. Cheianov, V. I. Fal'ko, K. Watanabe, T. Taniguchi, and R. V. Gorbachev, *Nat. Phys.* **7**, 958 (2011).
- [20] J. Xue, J. Sanchez-Yamagishi, D. Bulmash, P. Jacquod, A. Deshpande, K. Watanabe, T. Taniguchi, P. Jarillo-Herrero, and B. J. LeRoy, *Nat. Mater.* **10**, 282 (2011).
- [21] R. Decker, Y. Wang, V. W. Brar, W. Regan, H.-Z. Tsai, Q. Wu, W. Gannett, A. Zettl, and M. F. Crommie, *Nano Lett.* **11**, 2291 (2011).
- [22] C. R. Dean, L. Wang, P. Maher, C. Forsythe, F. Ghahari, Y. Gao, J. Katoch, M. Ishigami, P. Moon, M. Koshino, T. Taniguchi, K. Watanabe, K. L. Shepard, J. Hone, and P. Kim, *Nature (London)* **497**, 598 (2013).
- [23] J. C. Phillips, *Proc. Natl. Acad. Sci. USA* **105**, 9917 (2008).
- [24] P. J. Zomer, M. H. D. Guimarães, J. C. Brant, N. Tombros, and B. J. van Wees, *Appl. Phys. Lett.* **105**, 013101 (2014).
- [25] B. Karmakar, M. R. Gokhale, A. P. Shah, B. M. Arora, D. T. N. de Lang, A. de Visser, L. A. Ponomarenko, and A. M. M. Pruisken, *Physica E* **24**, 187 (2004).
- [26] C. Cobaleda, F. Rossella, S. Pezzini, E. Diez, V. Bellani, D. K. Maude, and P. Blake, *Physica E* **44**, 530 (2011).
- [27] C. Cobaleda, S. Pezzini, E. Diez, and V. Bellani, *Phys. Rev. B* **89**, 121404 (2014).
- [28] R. V. Gorbachev, F. V. Tikhonenko, A. S. Mayorov, D. W. Horsell, and A. K. Savchenko, *Phys. Rev. Lett.* **98**, 176805 (2007).
- [29] In order to determine L_ϕ , we fit the variation of the magnetoconductivity $\Delta\sigma_{xx}(B) \equiv \sigma_{xx}(B) - \sigma_{xx}(0)$ at a fixed value of V_g , to the expression given in Eq. (1) of Ref. [28]. Only the first two terms of the latter expression, involving the coherence time τ_ϕ and the intervalley scattering time τ_i , are considered for the fit.
- [30] The 95% confidence interval is obtained from the standard deviation of the sample mean of the set of κ values listed in Table I, multiplied by the appropriate factor given by the Student's t -distribution with six degrees of freedom.
- [31] F. V. Tikhonenko, D. W. Horsell, R. V. Gorbachev, and A. K. Savchenko, *Phys. Rev. Lett.* **100**, 056802 (2008).
- [32] S. Pezzini, C. Cobaleda, E. Diez, and V. Bellani, *Phys. Rev. B* **85**, 165451 (2012).
- [33] W. Pan, A. J. Ross, III, S. W. Howell, T. Ohta, T. A. Friedmann, and C.-T. Liang, *New J. Phys.* **13**, 113005 (2011).
- [34] S. A. Trugman, *Phys. Rev. B* **27**, 7539 (1983).
- [35] B. Kramer, T. Ohtsuki, and S. Kettemann, *Phys. Rep.* **417**, 211 (2005).
- [36] S. V. Morozov, K. S. Novoselov, M. I. Katsnelson, F. Schedin, D. C. Elias, J. A. Jaszczak, and A. K. Geim, *Phys. Rev. Lett.* **100**, 016602 (2008).
- [37] D. G. Polyakov and B. I. Shklovskii, *Phys. Rev. Lett.* **70**, 3796 (1993).
- [38] M. Furlan, *Phys. Rev. B* **57**, 14818 (1998).
- [39] F. Hohls, U. Zeitler, and R. J. Haug, *Phys. Rev. Lett.* **88**, 036802 (2002).
- [40] Using the expression $\sigma_{xx}(T) \propto e^{-(T/T_0)^\beta} / T$, we also checked that the best fits to our data occur for $\beta \approx 0.5$. Thus, VRH is the mechanism determining the broadening of σ_{xx} . See also Ref. [27].
- [41] M. Titov and M. I. Katsnelson, *Phys. Rev. Lett.* **113**, 096801 (2014).
- [42] M. Flöser, Ph.D. thesis, Université de Grenoble, 2012, <http://tel.archives-ouvertes.fr/tel-00866133>.